






IL-38 regulates intestinal stem cell homeostasis by inducing WNT signaling and beneficial IL-1 β secretion

Alberto Dinarello^{a,1}, Makenna May^{a,2}, Jesus Amo-Aparicio^{a,2}, Tania Azam^a, Joseph M. Gaballa^a, Carlo Marchetti^a , Annachiara Tesoriere^b, Rachele Ghirardo^c, Jasmina S. Redzic^c, William S. Webber III^a, Shaikh M. Atif^a, Suzhao Li^a , Elan Z. Eisenmesser^c, Dennis M. de Graaf^{a,3}, and Charles A. Dinarello^{a,4} 

Contributed by Charles A. Dinarello; received May 2, 2023; accepted September 13, 2023; reviewed by Gaby Palmer and Andreas Weigert

The IL-1 Family member IL-38 has been characterized primarily as an antiinflammatory cytokine in human and mouse models of systemic diseases. Here, we examined the role of IL-38 in the murine small intestine (SI). Immunostaining of SI revealed that IL-38 expression partially confines to intestinal stem cells. Cultures of intestinal organoids reveal IL-38 functions as a growth factor by increasing organoid size via inducing WNT3a. In contrast, organoids from IL-38-deficient mice develop more slowly. This reduction in size is likely due to the downregulation of intestinal stemness markers (i.e., *Fzd5*, *Ephb2*, and *Olfm4*) expression compared with wild-type organoids. The IL-38 binding to IL-1R6 and IL-1R9 is still a matter of debate. Therefore, to analyze the molecular mechanisms of IL-38 signaling, we also examined organoids from IL-1R9-deficient mice. Unexpectedly, these organoids, although significantly smaller than wild type, respond to IL-38, suggesting that IL-1R9 is not involved in IL-38 signaling in the stem cell crypt. Nevertheless, silencing of IL-1R6 disabled the organoid response to the growth property of IL-38, thus suggesting IL-1R6 as the main receptor used by IL-38 in the crypt compartment. In organoids from wild-type mice, IL-38 stimulation induced low concentrations of IL-1 β which contribute to organoid growth. However, high concentrations of IL-1 β have detrimental effects on the cultures that were prevented by treatment with recombinant IL-38. Overall, our data demonstrate an important regulatory function of IL-38 as a growth factor, and as an antiinflammatory molecule in the SI, maintaining homeostasis.

inflammation | interleukin | gastroenterology

The cytokine IL-38 belongs to the IL-1 family (1). It is encoded by the *Il1f10* gene and is expressed in infiltrating immune cells of colonic samples from patients with inflammatory bowel disease (IBD), particularly CD19⁺ B cells (2) and CD123⁺ cells (3). IL-38 is mostly studied as an antiinflammatory cytokine (1, 4) and exerts protective functions in several organs, suggesting that this protein mainly functions in the maintenance of organ homeostasis (1). As demonstrated by van de Veerdonk et al., IL-38 has biological effects in immune cells that resemble IL-36Ra functions, downregulating the levels of IL-22, IL-17, and IFN γ in *Candida*-stimulated Th17 cells (5). A recent study by The et al. also demonstrated that IL-38 dampens aortic valve calcification, probably dependent on IL-1R9 (encoded by *Il1rap1* gene), inhibiting Nucleotide-binding oligomerization domain-containing protein-like receptor (NLR) family pyrin domain containing 3 (NLRP3) and IL-1 β maturation (6). Moreover, *Il1f10*-deficient mice exhibit higher levels of inflammation when exposed to DSS treatment compared to wild-type mice and express higher levels of NLRP3 and caspase-1 (7). Regarding IBD, IL-38 is expressed in colon tissue of ulcerative colitis patients compared to healthy controls (8) and reduces inflammation in the colon (2).

Although most studies demonstrate that IL-38 has antiinflammatory properties by, for example, blocking IL-1 β maturation, the biological functions of IL-38 are more complex than only inhibiting the inflammatory response and some in vivo studies demonstrate that this cytokine favors disease progression. For instance, as shown in Huard et al. (9), IL-38 ablation in mice ameliorates autoimmune encephalomyelitis leading to the downregulation of inflammation markers like *Mertk*, *Tnfa*, *Ptgs2*, *Tgfb1*, and *Tgfb2* (9). Additionally, experiments performed on mouse and A431 human epidermoids cancer cell line reveal that IL-38 has a protumorigenic function and can stimulate cancer cell proliferation using an IL-1R6-dependent mechanism (10). Moreover, as regards keratinocytes differentiation, Mermoud et al. (11) have recently demonstrated that IL-38 is expressed in primary keratinocytes as well as in the N/TERT1 keratinocyte cell line. Notably, the overexpression of IL-38 promotes the differentiation of these cells, inhibiting proliferation (11).

Significance

The IL-1 family member IL-38 has been characterized primarily as an antiinflammatory cytokine for systemic diseases. Here, we describe a central role of IL-38 in driving intestinal stem cell differentiation through the upregulation of WNT3a and IL-1 β . Our findings reveal a dual role of IL-38 in regulating intestinal functions; a) in resting conditions, IL-38 maintains intestinal homeostasis, driving WNT3a production and organoid budding, whereas b) in highly inflamed conditions, IL-38 contributes to proper recovery, by exerting antiinflammatory activities. Thus, we demonstrate a pivotal role of IL-38 in driving tissue turnover and maintenance of homeostasis in intestinal health.

Reviewers: G.P., Universite de Geneve; and A.W., Goethe-University Frankfurt.

The authors declare no competing interest.

Copyright © 2023 the Author(s). Published by PNAS. This article is distributed under [Creative Commons Attribution-NonCommercial-NoDerivatives License 4.0 \(CC BY-NC-ND\)](https://creativecommons.org/licenses/by-nc-nd/4.0/).

¹Present address: Novo Nordisk Foundation Center for Stem Cell Medicine (reNEW), University of Copenhagen, Copenhagen DK-2200, Denmark.

²M.M. and J.A.-A. contributed equally to this work.

³Present address: Department for Innate Immunity and Metaflammation, Institute of Innate Immunity, University Hospital Bonn Biomedical Center, Bonn 53127, Germany.

⁴To whom correspondence may be addressed. Email: charlesdinarello@gmail.com.

This article contains supporting information online at <https://www.pnas.org/lookup/suppl/doi:10.1073/pnas.2306476120/-/DCSupplemental>.

Published October 31, 2023.

Another debated aspect of IL-38 biology relates to the identity of its receptor. As previously proposed by van de Veerdonk et al. (5), IL-38 binds IL-36R (IL-1R6) which is encoded by the *Il1rl2* gene. Other evidence regarding the interaction of IL-38 with IL-1R6 comes from Mora et al. (12), who demonstrated that IL-38 binds either IL-1R6 or IL-1R9 (12). Additionally, pulldown experiments performed by Zhou et al. (10) support the IL-38–IL-1R6 interaction. IL-38 may also bind IL-1R1 and the affinity of interaction depends on the truncation of the N-terminal amino acids of IL-38 (13).

Given the emerging importance of a therapeutic role for IL-38 (14–16) and the function of this cytokine in the intestine (2, 7, 8, 17), here we analyzed the effects of IL-38 in intestinal stem cells (ISCs) in organoid cultures derived from wild-type and *Il1f10* mice. Moreover, to better dissect the mechanism of action of IL-38 in the gut, we employed *Il1rap1l*-deficient mice and observed that IL-1R9 is not essential for a response to IL-38. Additionally, silencing experiments highlight the role of IL-1R6 in IL-38 signaling. Moreover, we presented that IL-38 induces low concentrations of IL-1 β . This finding, confirmed in *Il1r1* and *Nlrp3*-deficient mice, reveals that homeostatic levels of IL-1 β are beneficial for organoids.

Results

***Il1f10*-Deficient SI Shows Lower Expression of Intestinal Stem Cell Markers.** Located in the intestinal crypts, ISCs represent the precursor cells of the entire intestine (18). These cells regulate homeostasis of the intestine, producing soluble factors that affect the fate of the intestine. The crypts are divided into two zones: the stem cell zone and the transient applying zone (TA). The stem cell zone contains the crypt base columnar cells that act as ISCs, as well as Paneth cells that protect and feed the ISCs (19). The TA zone is composed by lineage-committed stem cells, which rapidly divide and differentiate; the mature cell zone is populated by large numbers of epithelial cells (19). To determine these areas, cell markers have been identified to show differentiated and undifferentiated cells. Historically, the most important marker of ISCs is LGR5 (18, 20–22), a G-protein-coupled receptor and a target of the WNT pathway (23). As demonstrated by Carmon et al., LGR5 binds R-spondins for enhancing the activation of the WNT/ β -catenin signaling in WNT-responsive cells (24). The WNT/ β -catenin axis is fundamental for crypt homeostasis and maintains ISCs in an undifferentiated state (21); however, WNT/ β -catenin signaling can also drive the differentiation of ISCs in Paneth cells (25).

IL-38 is an antiinflammatory cytokine that can protect the organism challenged with highly inflammatory triggers, as recently observed in dextran sodium sulfate colitis or aortic calcification models (6, 7). We sought to confirm whether IL-38 is expressed in the mouse intestine (8) and if the IL-38 protein is expressed in the small intestine (SI) at the level of the stem cell crypts. As shown in Fig. 1*A* and *SI Appendix, Fig. S1G*, IL-38 staining colocalizes with LGR5 staining, revealing that IL-38 is expressed in stem cell crypts and suggesting a role of this cytokine in ISCs. IL-38 gene (*Il1f10*) expression in the SI is markedly lower when compared to a high *Il1f10*-expressing tissue like skin, probably because intestinal IL-38 expression is specifically localized in a small SI stem cell crypt subpopulation (Fig. 1*B*).

To confirm the putative contribution of IL-38 to homeostasis of ISCs, we analyzed the intestinal histology and compared wild type with *Il1f10*^{-/-} mice. Longitudinal histological sections shown in *SI Appendix, Fig. S1 A–F* did not reveal overt structural differences between the two experimental groups in healthy conditions. Therefore, we decided to analyze whether some intestinal fundamental pathways are transcriptionally impaired in the knockouts compared to the wild type. First, we measured the level of expression of

stem cell niche markers (taken from refs. 26 and 27) in SIs samples from wild-type and *Il1f10*-deficient mice. Among the markers analyzed, *Fzd5*, *Ephb2*, *Bmpr1a*, *Clca4*, *Pdgfra*, *Olfm4*, *Smoc2*, *Socs3*, *Cdk6*, *Phlda*, and *Pla2g4a* are significantly down-regulated in *Il1f10*-deficient mice compared to wild type (Fig. 1 *C–W*), demonstrating the pivotal role of IL-38 in intestinal stem cell niche gene expression. These findings are further corroborated by western blot of intestinal extracts against LGR5. As shown in *SI Appendix, Fig. S1 H and I*, LGR5 expression is significantly reduced in *Il1f10*-deficient intestines compared to wild type. We then decided to analyze the expression levels of other genes involved in intestinal regeneration (28, 29) such as *Clu*, *Ly64*, *Anxa8*, *Ereg*, *Rxna*, *Il33*, *Tacstd2*, and *Mlsn* in wild-type intestines compared to *Il1f10*^{-/-}-deficient ones. Among these transcripts, only *Ly64* resulted up-regulated in IL-38 knockout samples, suggesting for an impairment of intestinal barrier functions due to IL-38 loss (*SI Appendix, Fig. S2 A–H*).

Additionally, we decided to analyze the level of expression of several IL-encoding genes, to see whether IL-38 deficiency leads to an impairment in ILs expression. As reported in *SI Appendix, Fig. S3 A–E*, *Il36a*, *Il36b*, *Il36g*, *Il36rn*, and *Il1b* (encoding, respectively, for IL-36 α , IL-36 β , IL-36 γ and IL-36RA and IL-1 β) are not differentially expressed in wild-type intestines when compared to *Il1f10* knockout. We also measured the intracellular levels of IL- β in the intestines from wild-type and *Il1f10*-deficient mice and we did not observe statistical differences between the two experimental groups (*SI Appendix, Fig. S3F*). To confirm that IL-38 does not influence the expression of IL-36 genes, we injected 1 μ g of recombinant mouse IL-38 (3 to 152 residues) in wild-type mice every day for 15 d. At the end of the experiment, we collected the intestines from Phosphate buffer saline (PBS)-injected controls (Vehicle) and from IL-38-injected animals and we measured the expression of *Il36a*, *Il36b*, *Il36g*, and *Il36rn*. As reported in *SI Appendix, Fig. S4 A–D*, IL-38 injection did not affect the expression of these genes, suggesting that, at least in this context, IL-38 does not induce IL-36 gene expression.

IL-38 Is a Growth Factor in Intestinal Organoids. To test the functions of IL-38 ex vivo, we generated organoid cultures from wild-type SI. Organoids were stimulated with recombinant mouse IL-38 (3 to 152 residues) at three different concentrations. Interestingly, 2 ng/mL and 200 ng/mL did not affect organoid size (*SI Appendix, Fig. S4 E–H*) ($P = 0.2314$ and 0.9996 , respectively), whereas 20 ng/mL of IL-38 increased the size of organoids (Fig. 2 *A* and *B*) ($P = 0.0239$). Additionally, we injected 1 μ g recombinant mouse IL-38 in wild-type mice every day for 15 d and collected SI to generate organoid cultures. Notably, organoids obtained from IL-38-injected mice are larger than vehicle-injected mice ($P = 0.0459$), confirming that IL-38 can function as a growth factor in healthy in vivo intestines (Fig. 2 *C* and *D*).

WNT3a is the major soluble factor produced by Paneth cells that drives ISCs differentiation (24). To understand how IL-38 affects organoid growth, we measured the levels of WNT3a in organoids. As shown in Fig. 2*F*, we observed a significant increase with IL-38 stimulation (1,500-fold increase, $P < 0.001$) (Fig. 2*E*). To confirm whether the increase of organoid size depends on IL-38-induced WNT3a secretion, we treated organoids with the WNT inhibitor IWP4 (30) either with or without IL-38 stimulation. As expected, IL-38 stimulated organoid growth ($P = 0.0082$), whereas IWP4 did not affect organoid size compared to vehicle yet changed the organoid shape (Fig. 2*F* and *G*). Moreover, organoids treated with IL-38 and IWP4 combination do not show significant differences when compared to either vehicle ($P = 0.9962$) or IWP4-treated ($P = 9988$) organoids but are significantly smaller compared to IL-38-treated organoids (Fig. 2*F* and *G*). Furthermore, we observed the same phenotype in organoids treated with IWP4 and IL-38+IWP4 (Fig. 2

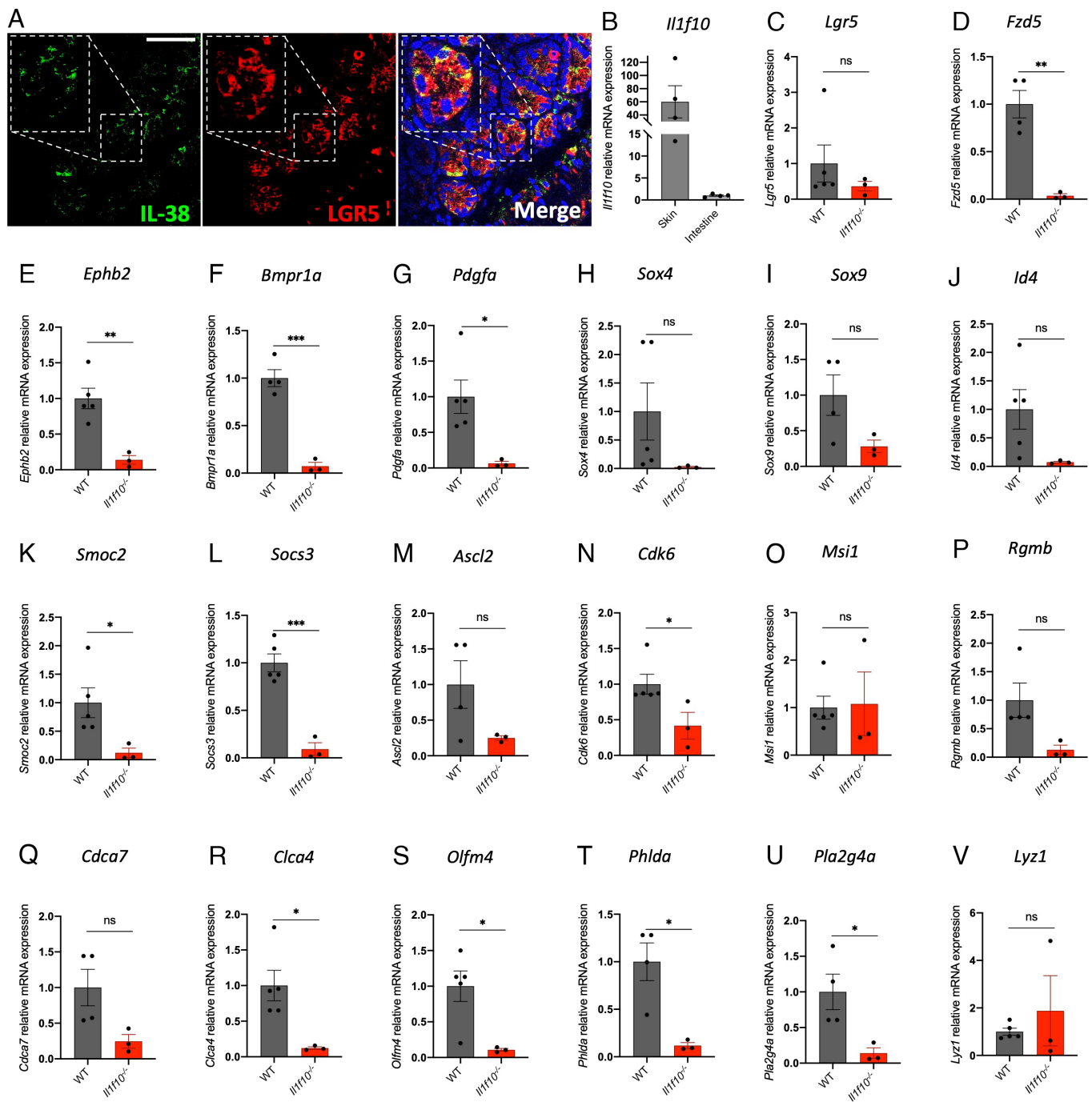


Fig. 1. IL-38 is essential for intestinal crypt gene expression. (A) Staining of IL-38 (green) and LGR5 (red) in wild-type SI. An enlargement of one intestinal crypt is shown in dashed frame. (Scale bar, 50 μ m.) (B) Gene expression of *Il1f10* in skin and intestine of wild-type mice. (C–V) Gene expression analysis of *Lgr5* (C), *Fzd5* (D), *Ephb2* (E), *Bmpr1a* (F), *Pdgfra* (G), *Sox4* (H), *Sox9* (I), *Id4* (J), *Smoc2* (K), *Socs3* (L), *Ascl2* (M), *Cdk6* (N), *Msi1* (O), *Rgmb* (P), *Cdca7* (Q), *Clca4* (R), *Olfm4* (S), *Phlda* (T), *Pla2g4a* (U), and *Lyz1* (V) in SIs of wild-type and *Il1f10*-deficient mice. Comparisons between WT and *Il1f10* knockout samples were performed using Student *t* test. * $P < 0.05$; ** $P < 0.01$; *** $P < 0.001$, ns = not significant. Mean \pm SEM.

F and G). These data suggest that IL-38 stimulates organoid growth by inducing WNT3a production and that these effects are dependent on the WNT pathway. To confirm the actual inhibition of WNT pathway, we also measured the expression of WNT and stemness marker genes and we observed that *Lgr5*, *Lyz1*, and *Olfm4* are significantly down-regulated in IWP4-treated organoids compared to control and IL-38-treated organoids (Fig. 2 H–K).

***Il1f10*-Deficient (*Il1f10*^{-/-}) Organoids Show Growth Defects.** Organoid cultures from wild-type and IL-38-deficient mice (*Il1f10*^{-/-}) were evaluated for growth. IL-38-deficient organoids

are significantly smaller than wild-type organoids ($P = 0.0135$) and, as expected, 20 ng/mL recombinant IL-38 significantly increased the size of either wild-type ($P = 0.0497$) or IL-38-deficient organoids (0.0210) (Fig. 3 A and B).

Interestingly, we observed a marked downregulation of stemness markers in *Il1f10* knockout organoids compared to wild type. *Lgr5* does not show significant differences between *Il1f10*^{-/-} and wild-type organoids, whereas *Fzd5*, *Ephb2*, and *Olfm4* are significantly down-regulated in *Il1f10*-deficient organoids when compared to wild type ($P = 0.9763$, 0.0208, 0.0076, and 0.0091, respectively) (Fig. 3 C–F).

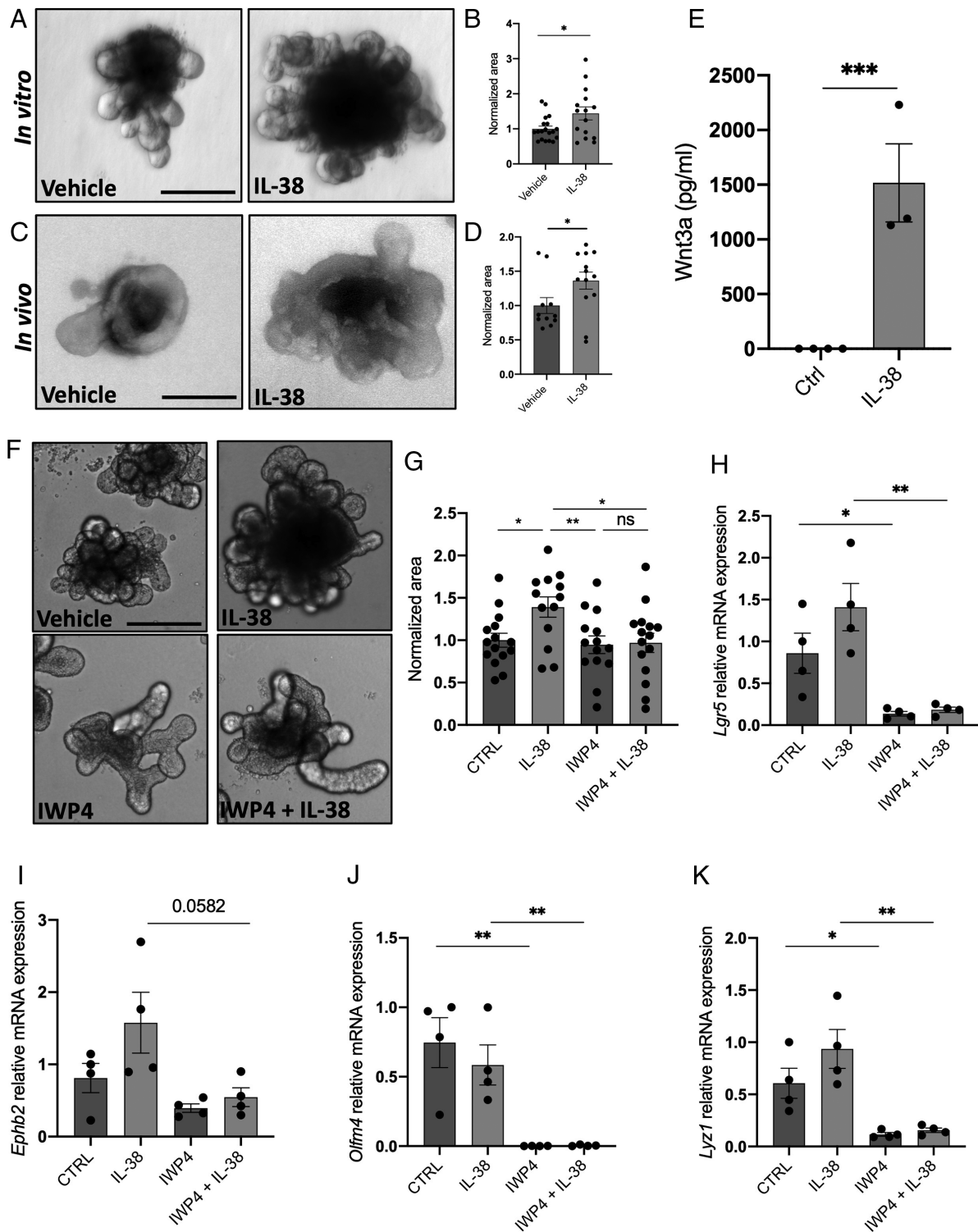


Fig. 2. IL-38 works as a growth factor stimulating WNT3a secretion. (A) Representative pictures and (B) measurement of wild-type organoids treated with 20 ng/mL IL-38 for 6 d. Each dot represents an individual organoid, organoid cultures were produced from 3 different mice and plated in three wells for each experimental condition. (Scale bar: 200 μ m.) Comparisons between control and IL-38-treated organoids were performed using Student *t* test. (C) Representative pictures and (D) measurements of wild-type organoids obtained from vehicle- and IL-38-injected mice. PSB or 1 μ g recombinant murine IL-38 was intraperitoneally injected every day for 15 d. Each dot represents an individual organoid, organoid cultures were produced from 5 different mice per condition and plated in three wells for each experimental condition. (Scale bar: 200 μ m.) Comparisons between control and IL-38-treated organoids were performed using Student *t* test. (E) WNT3a expression in the supernatants in wild-type organoids treated with 20 ng/mL IL-38 for 6 d. Comparisons between control and IL-38-treated organoids were performed using Student *t* test. (F) Representative pictures and (G) measurement of wild-type organoids treated with vehicle, 20 ng/mL IL-38, 5 μ M IWP4, and 5 μ M IWP4 + 20 ng/mL IL-38. Each dot represents an individual organoid, organoid cultures were produced from 3 different mice and plated in three wells for each experimental condition. (Scale bar: 200 μ m.) Comparisons between the four experimental groups were performed using one-way ANOVA. (H–K) Gene expression of *Lgr5* (H), *Ephb2* (I), *Olfm4* (J), and *Lyz1* (K) in wild-type organoids treated with vehicle, 20 ng/mL IL-38, 5 μ M IWP4, and 5 μ M IWP4 + 20 ng/mL IL-38. **P* < 0.05; ***P* < 0.01, ****P* < 0.001, ns = not significant. Mean \pm SEM.

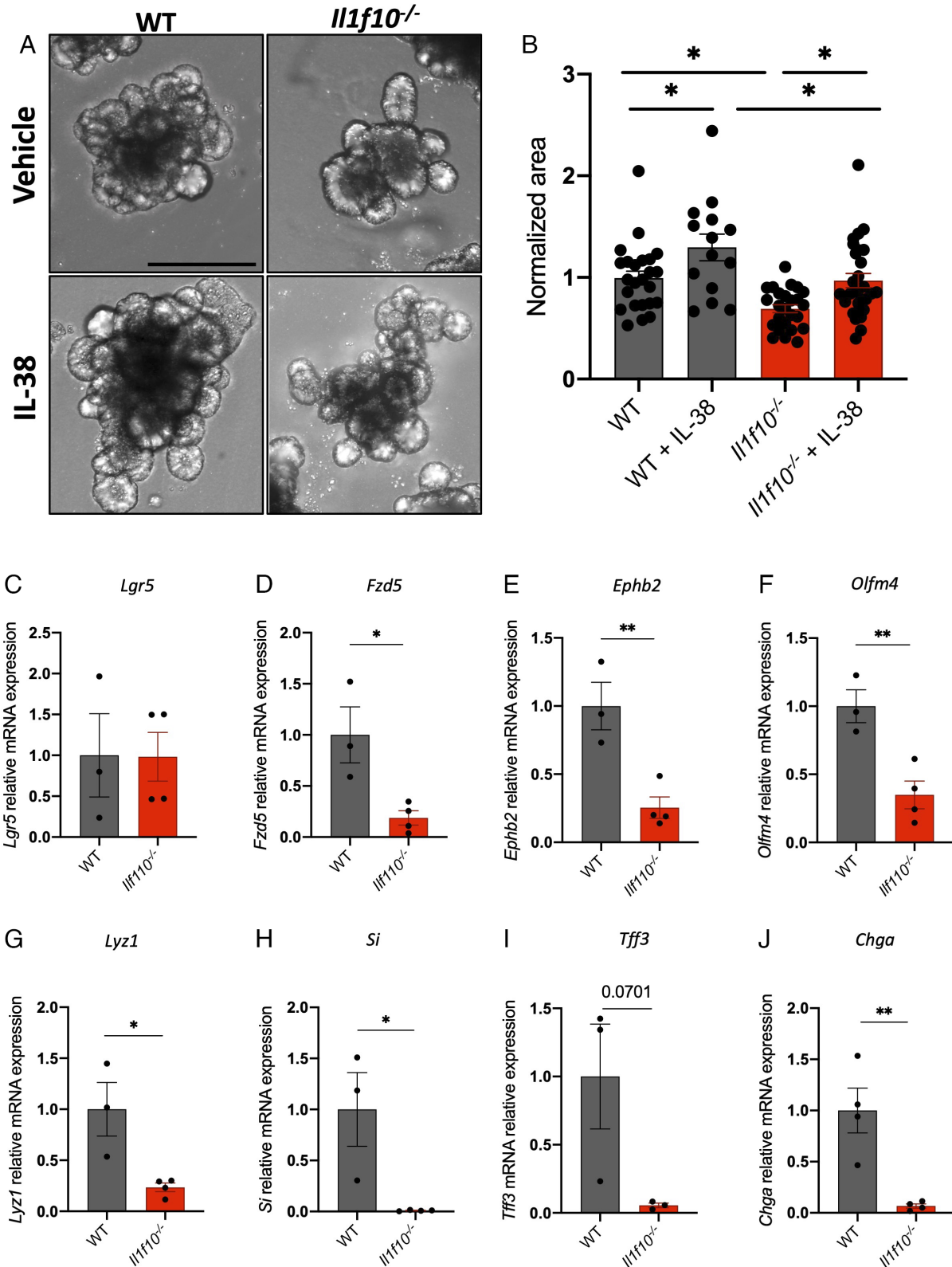


Fig. 3. *I1f10*-deficient organoids show growth defects. (A) Representative pictures and (B) measurements of wild-type and *I1f10*^{-/-} organoids treated either with vehicle or 20 ng/mL IL-38 for 6 d. Each dot represents an individual organoid, organoid cultures were produced from 3 different mice and plated in three wells for each experimental condition. (Scale bar: 200 μ m.) Comparisons between the four experimental groups were performed using one-way ANOVA. (C–J) Gene expression analysis of *Lgr5* (C), *Fzd5* (D), *Ephb2* (E), *Olfm4* (F), *Lyz1* (G), *Si* (H), *Tff3* (I), and *Chga* (J) in wild-type and *I1f10*^{-/-} organoids. Comparisons between WT and *I1f10* knockout samples were performed using Student *t* test. **P* < 0.05; ***P* < 0.01, *****P* < 0.0001. Mean \pm SEM.

To further characterize *I1f10*^{-/-} organoids, we measured the levels of expression of markers of other cell types such as *Lyz1* (Paneth cells), *Si* (absorptive cells), *Tff3* (goblet cells), and *Chga*

(goblet cells) (31). Notably, all these markers were down-regulated in *I1f10*-deficient organoids (*P* = 0.0195, 0.0217, 0.0701, and 0.0055, respectively), suggesting that the lack of IL-38 fundamentally

affects the differentiation of ISC through several intestinal cell types (Fig. 3 G–J).

***Il1rap1*-Deficient (*Il1rap1*^{-/-}) Organoids Show Growth Defects.** IL-38 functions are determined by its interaction with its putative receptors IL-1R6 and IL-1R9 (5, 10, 12, 13).

Using RNA extracted from wild-type and *Il1rap1*-deficient SIs, we demonstrated that, among all the transcripts analyzed in Fig. 1, *Fzd5*, *Bmpr1a*, *Cdca7*, and *Phlda* are significantly down-regulated in *Il1rap1*-deficient intestines compared to wild-type controls (Fig. 4 A–D). In contrast, other genes are not differentially expressed between wild-type and *Il1rap1*-deficient intestines, whereas *Cla4* was significantly up-regulated (SI Appendix, Fig. S5 A–O). These observations suggest that IL-1R9 is involved in the correct intestinal stem cell niche homeostasis, but its absence impacts stemness markers less than IL-38 deficiency.

Next, we cultured organoids derived from wild-type and *Il1rap1*-deficient mice and we observed that *Il1rap1* knockout organoids are significantly smaller than wild-type-derived organoids ($P = 0.0249$), highlighting the importance of IL-1R9 in intestinal stem cell niche homeostasis (Fig. 4 E and F). Moreover, IL-38 stimulation of organoid cultures revealed that both wild-type and *Il1rap1*-deficient cultures ($P = 0.0001$) respond to stimulation. In fact, we observed a significant increase of organoid size in IL-38-treated wild-type ($P = 0.0328$) and *Il1rap1*-deficient organoids ($P = 0.0001$) compared to untreated controls (Fig. 4 E and F). In addition, RT-qPCR for *Lgr5*, *Fzd5*, *Ephb2*, *Olfm4*, and *Lyz1* revealed no differences between wild-type and *Il1rap1* KO organoids (Fig. 4 G–K). These data demonstrate that IL-1R9 is not required for IL-38 biological activities in intestinal organoids and that another receptor is involved in IL-38-signaling.

IL-1R6 Is Involved in IL-38 Signaling in the Intestinal Crypt. IL-1R6 is encoded by the *Il1rl2* gene. In order to understand whether the lack of this receptor has a detrimental effect on organoid growth, we used *Il1rl2* siRNAs on wild-type organoids. As shown in Fig. 5 A and B, *Il1rl2* silencing determines a significant reduction of organoid size ($P < 0.0001$), suggesting an important role of IL-1R6 in this process. After validating *Il1rl2* RNA silencing by RT-qPCR (Fig. 5 C) ($P = 0.0218$), we measured the expression levels of *Lgr5*, *Fzd5*, *Ephb2*, *Olfm4*, and *Lyz1*. Differently to what we observed with *Il1rap1*-deficient organoids, *Il1rl2* silencing resulted in a significant downregulation of *Fzd5* and *Ephb2* ($P = 0.0113$ and 0.0074 , respectively), without significantly affecting the expression of the other markers analyzed (Fig. 5 D–H).

Next, we sought to assess whether organoids can respond to IL-38 even in the absence of IL-1R6. To do so, we incubated wild-type organoids with either control siRNA or *Il1rl2* siRNA and we stimulated them for 6 d with IL-38. As observed in Fig. 5 I and J, recombinant IL-38 significantly increases the organoid size in control siRNA-treated organoids ($P < 0.0001$), but we could not see significant differences between *Il1rl2*-silenced organoids treated with vehicle or with recombinant IL-38 ($P > 0.999$), suggesting that IL-38 increases organoid growth through IL-1R6. To better evaluate the role of IL-1R6 and IL-1R9 in IL-38 biological activity, we silenced *Il1rl2* in *Il1rap1*-deficient organoids. As previously observed in Fig. 4 E and F, *Il1rap1*-deficient organoids indeed respond to IL-38 ($P < 0.0001$); however, upon silencing with *Il1rl2* siRNA, IL-38 did not stimulate growth ($P > 0.999$) (Fig. 5 I and J). These data demonstrate that IL-38 signaling depends on IL-1R6, whereas IL-1R9 plays a separate role in intestinal organoid homeostasis.

Low Concentrations of IL-1 β Stimulate Organoid Growth. Together with the induction of WNT3a in organoid supernatants (as observed in Fig. 2), IL-38 induces a low but significant

concentration of IL-1 β (about 25 pg/mL; $P < 0.0001$) (Fig. 6A), suggesting a possible role of this cytokine in the correct homeostasis of organoids. To test the importance of IL-1 β in intestinal organoid cultures, we first decided to block IL-1 signaling by treating wild-type organoids with 10 μ g/mL Anakinra (a commercially available antagonist of IL-1 receptor) for 6 d. Anakinra significantly reduces organoids size ($P < 0.0001$), suggesting the importance of IL-1 signaling for the proper development of intestinal cells (Fig. 6 B and C). To confirm this result, we generated cultures of *Il1r1* knockout organoids. As observed in Fig. 6 D and E, *Il1r1*-deficient organoids are significantly smaller than wild type ($P < 0.0001$), recapitulating with a genetic model what we previously observed with Anakinra treatment (Fig. 6 B–E). Similarly, *Nlrp3* knockout organoids, that do not produce NLRP3, fundamental for inflammasome formation thus for the conversion of pro-IL-1 β into mature IL-1 β (32), show a marked reduction in size when compared to wild type ($P < 0.0001$) (Fig. 6 F and G). These data demonstrate a central role of IL-1 β in organoid growth.

Since we observed that IL-38 induces low concentrations of IL-1 β (Fig. 6A), we decided to test the response of organoids to different concentrations of this cytokine. As also observed by Katsura et al. in lung organoids (33), low concentrations (10 pg/mL) of IL-1 β stimulate organoid growth ($P = 0.0076$) (Fig. 6 H and I). Notably, higher concentrations do not affect organoid size possibly because of IL-1 β -dependent cytotoxicity (Fig. 6 H and I). The highest IL-1 β concentration used (10 ng/mL), on the other hand, probably inducing cell death in the organoids, significantly reduced their size ($P = 0.0485$) (Fig. 6 J and K). The protective functions of IL-38 against high levels of IL-1 β are confirmed by treating wild-type organoids with 20 ng/mL IL-38 and 10 ng/mL IL-1 β . Organoids treated with 20 ng/mL IL-38 and 10 ng/mL IL-1 β are significantly larger than 10 ng/mL IL-1 β -treated organoids ($P = 0.0028$) and do not appear significantly different to vehicle organoids ($P = 0.5736$) (Fig. 6 J and K).

Another confirmation of the protective role of IL-38 was obtained from LPS-treated cultures. LPS exerts detrimental effects on organoid growth (34) (SI Appendix, Fig. S6 A and B). Therefore, we tested three concentrations of LPS (10, 100, and 1,000 ng/mL) and we observed a nonsignificant trend of reduction in organoid size upon 10 ng/mL LPS treatment compared to untreated organoids ($P = 0.982$), whereas 100 and 1,000 ng/mL significantly reduced organoid size compared to untreated controls ($P = 0.0027$ and 0.0002 , respectively) (SI Appendix, Fig. S6 A and B). To test the protective effects of IL-38, we treated organoids with 100 ng/mL LPS with or without the presence of 20 ng/mL IL-38. While LPS decreases organoid size ($P = 0.0139$) and IL-38 alone increases size ($P = 0.039$), IL-38 rescues LPS-dependent negative effects ($P = 0.0113$) (SI Appendix, Fig. S6 C and D).

Discussion

Several studies highlight the role of interleukins in regulating intestinal crypt functions. For instance, IL-22 protects ISCs from immune-mediated tissue damage and promotes intestinal epithelial regeneration (35, 36). Additionally, IL-22, by activating the STAT3 pathway and inhibiting WNT and Notch signaling, suppresses cell differentiation and intestinal stem cell self-renewal (37). However, a study of human intestinal organoids has recently highlighted the role of IL-22 in the maturation of Paneth cells (38). Similar effects on cell differentiation were observed by Deng et al. in their report on IL-10, which leads to inhibition of the WNT pathway and the subsequent depletion of ISCs (39). On the other hand, the chronic exposure of IL-1 β

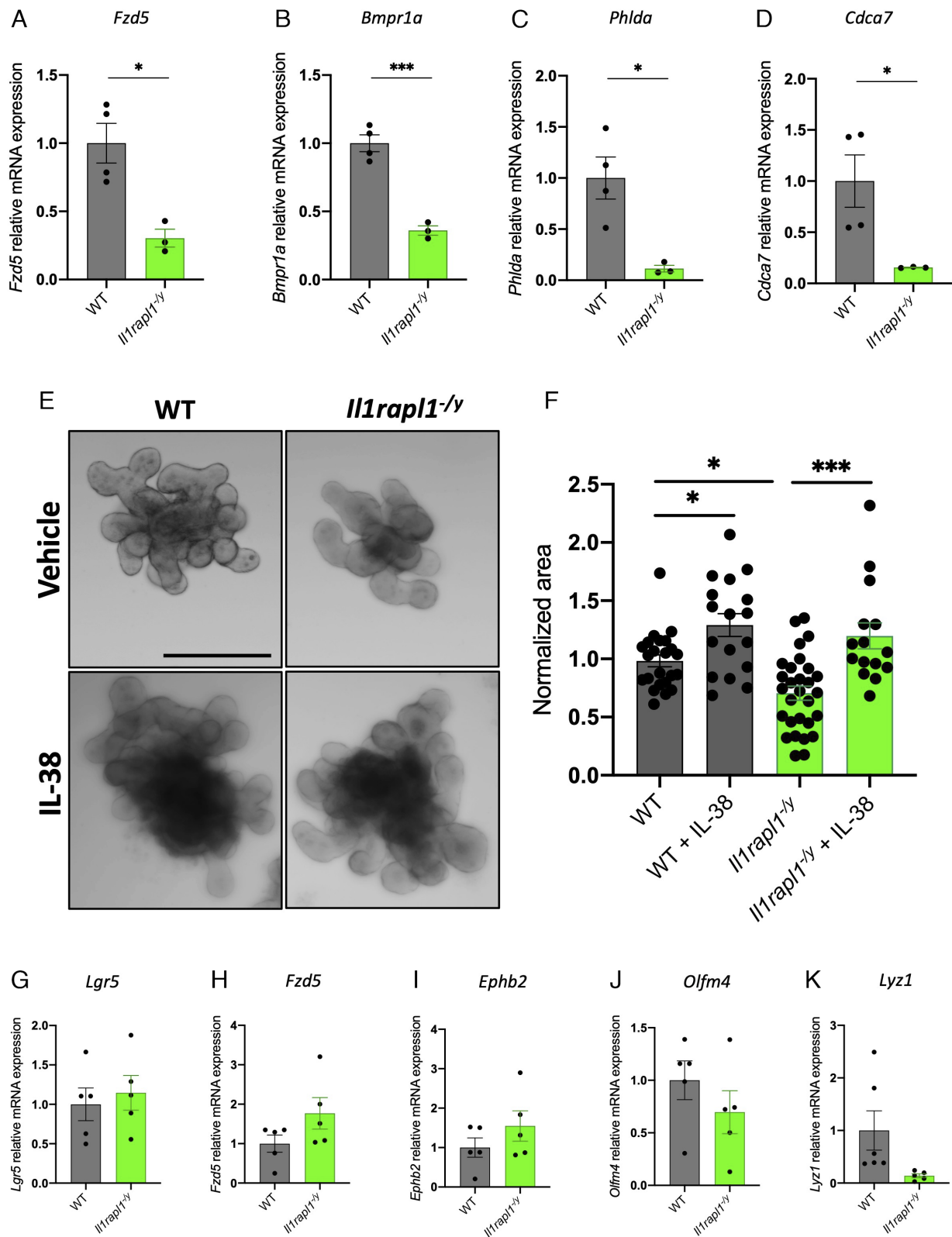


Fig. 4. *Il1rap1*-deficient organoids show growth defects. (A–D) Gene expression analysis of *Fzd5* (A), *Bmpr1a* (B), *Phlda* (C), and *Cdca7* (D) in SI of wild-type and *Il1rap1*-deficient mice. Comparisons between WT and *Il1rap1* knockout samples were performed using Student *t* test. (E) Representative pictures and (F) measurements of wild-type and *Il1rap1*-deficient organoids treated either with vehicle or 20 ng/mL IL-38 for 6 d. Each dot represents an individual organoid, organoid cultures were produced from 3 different mice and plated in three wells for each experimental condition. (Scale bar: 200 μ m.) Comparisons between the four experimental groups were performed using one-way ANOVA. (G–K) Gene expression analysis of *Lgr5* (G), *Fzd5* (H), *Ephb2* (I), *Olfm4* (J), and *Lyz1* (K) in wild-type and *Il1rap1*-deficient organoids. Comparisons between WT and *Il1rap1* knockout samples were performed using Student *t* test. * $P < 0.05$; ** $P < 0.01$. Mean \pm SEM.

induces the expression of stem cell markers like *Bmi1*, *Lgr5*, *c-Myc*, β -*catenin*, and *Nanog* in the IEC-18 rat epithelial cell line, showing a putative role of this cytokine in stem cell homeostasis

(40). Additionally, IL-33, deriving from pericryptal fibroblasts, drives intestinal differentiation, inducing the expansion of secretory cells (41).

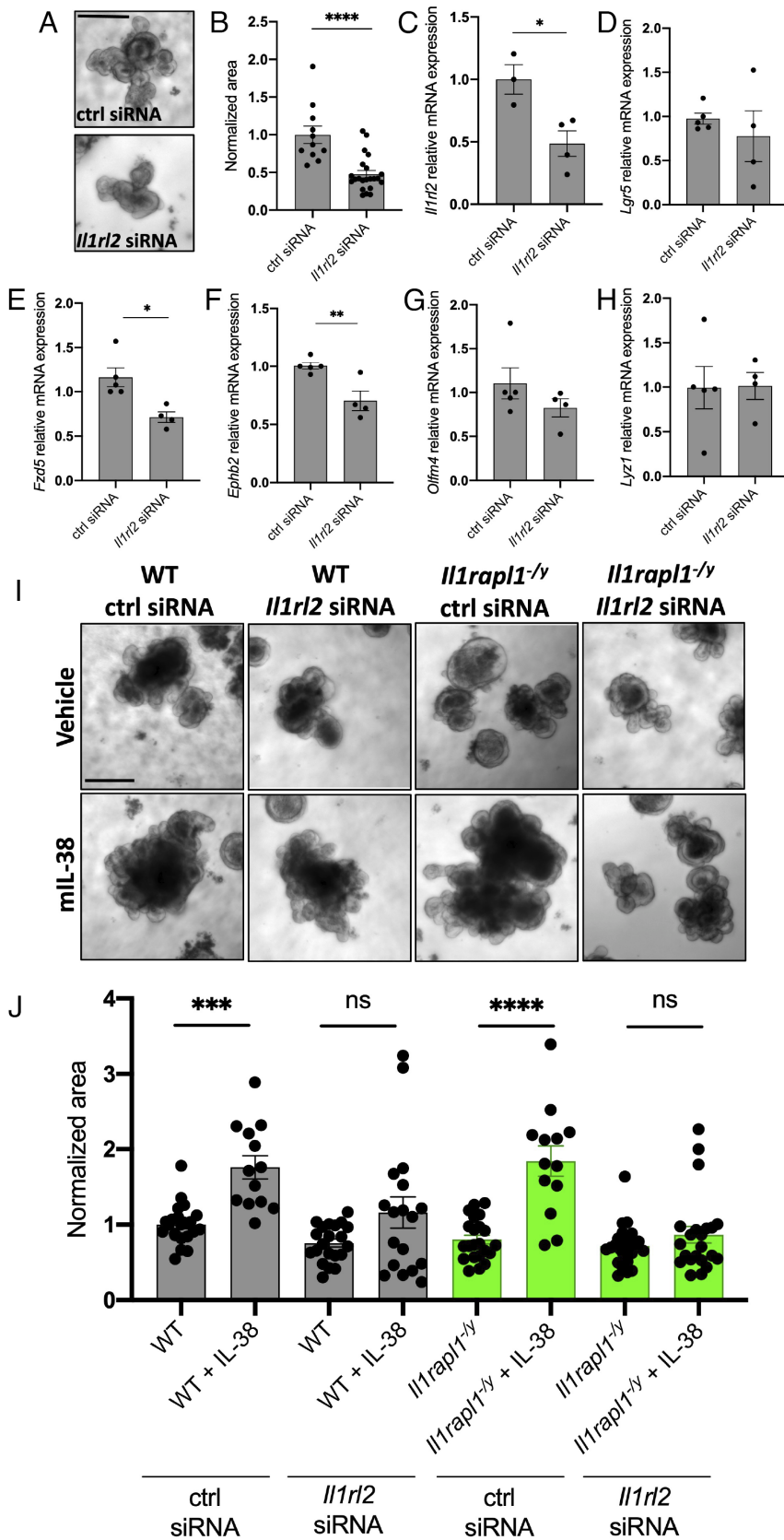


Fig. 5. *Il1rl2* silencing negatively affects organoid growth. (A) Representative pictures and (B) measurements of wild-type organoids treated with control siRNA or *Il1rl2* siRNA for 6 d. Each dot represents an individual organoid; organoid cultures were produced from 3 different mice and plated in three wells for each experimental condition. (Scale bar: 200 μ m.) Comparisons between control siRNA and *Il1rl2* siRNA organoids were performed using Student *t* test. (C–H) Gene expression analysis of *Il1rl2* (C), *Lgr5* (D), *Fzd5* (E), *Ephb2* (F), *Olfm4* (G), and *Lyz1* (H) in wild-type organoids treated with either control siRNA or *Il1rl2* siRNA for 6 d. Comparisons between control siRNA and *Il1rl2* siRNA organoids were performed using Student *t* test. (I) Representative pictures and (J) measurements of wild-type and *Il1rap1*-deficient organoids treated with control siRNA, *Il1rl2* siRNA, vehicle, or IL-38 for 6 d. Each dot represents an individual organoid; organoid cultures were produced from 3 different mice and plated in three wells for each experimental condition. (Scale bar: 200 μ m.) Comparisons between the eight experimental groups were performed using one-way ANOVA. * $P < 0.05$; ** $P < 0.01$; **** $P < 0.0001$. Mean \pm SEM.

In the present studies, we analyzed the role of IL-38, in order to better define its functions in the gut, including the downstream molecular mechanisms that IL-38 activates to maintain the homeostasis of intestinal tissue. We know that IL-38 reduces intestinal inflammation, and the lack of this cytokine hampers gut recovery

after DSS-induced injury (2, 7, 8). Therefore, we focused on the stem cell compartment in intestinal crypt. We demonstrated that exogenous IL-38 stimulation induced the activation of WNT pathway triggering the secretion of the agonist WNT3a, which resulted in the increase of organoid size and budding. On the other hand,

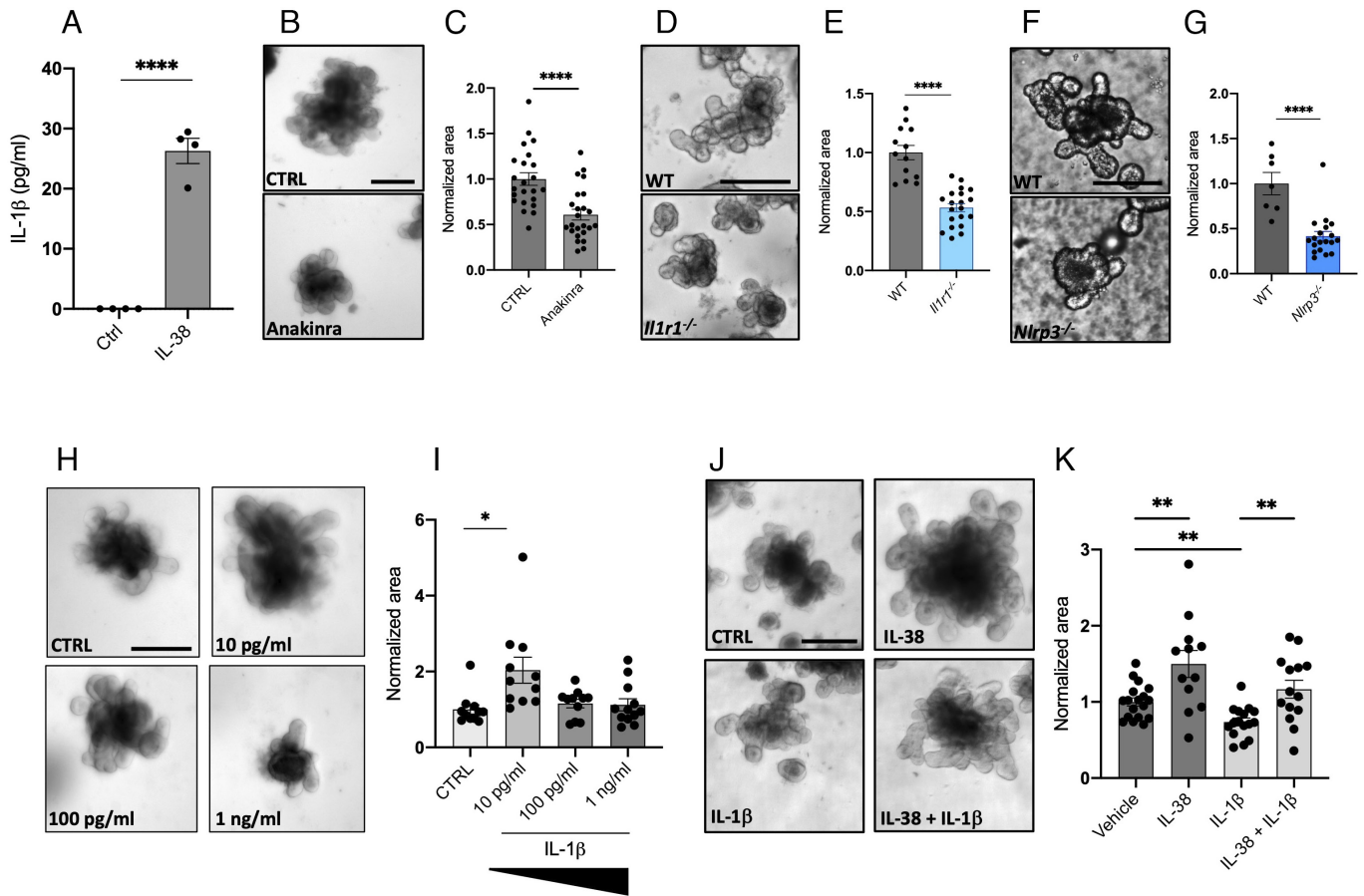


Fig. 6. Low concentrations of IL-1 β induce organoid growth. (A) IL-1 β expression in the supernatants in wild-type organoids treated with 20 ng/mL IL-38 for 6 d. Comparisons between control and IL-38-treated organoids were performed using Student *t* test. (B) Representative pictures and (C) measurements of wild-type organoids treated with 10 μ g/mL Anakinra for 6 d. Each dot represents an individual organoid, organoid cultures were produced from 3 different mice and plated in three wells for each experimental condition. (Scale bar: 200 μ m.) Comparisons between control and Anakinra-treated organoids were performed using Student *t* test. (D) Representative pictures and (E) measurement of wild-type and *Il1r1*^{-/-} organoids. Each dot represents an individual organoid; organoid cultures were produced from 3 different mice and plated in three wells for each experimental condition. (Scale bar: 200 μ m.) Comparisons between control and *Il1r1* knockout organoids were performed using Student *t* test. (F) Representative pictures and (G) measurement of wild type and *Nlrp3*^{-/-} organoids. Each dot represents an individual organoid; organoid cultures were produced from 3 different mice and plated in three wells for each experimental condition. (Scale bar: 200 μ m.) Comparisons between control and *Nlrp3* knockout organoids were performed using Student *t* test. (H) Representative pictures and (I) measurements of wild-type organoids treated with 10 pg/mL, 100 pg/mL and 1 ng/mL IL-1 β for 6 d. Each dot represents an individual organoid, organoid cultures were produced from 3 different mice and plated in three wells for each experimental condition. (Scale bar: 200 μ m.) Comparisons between the four experimental groups were performed using one-way ANOVA. (J) Representative pictures and (K) measurements of wild-type organoids treated with vehicle, 20 ng/mL IL-38, 10 ng/mL IL-1 β , and 20 ng/mL IL-38 + 10 ng/mL IL-1 β for 6 d. Each dot represents an individual organoid, organoid cultures were produced from 3 different mice and plated in three wells for each experimental condition. (Scale bar: 200 μ m.) Comparisons between the four experimental groups were performed using one-way ANOVA. **P* < 0.05; ***P* < 0.01; *****P* < 0.0001. Mean \pm SEM.

genetic ablation of IL-38 resulted in the downregulation of several stem cell markers (*Fzd5*, *Ephb2*, *Olfm4*). These markers are usually related to stemness and WNT activity (42–44). In addition, IL-38 deficiency also severely dampened the expression of markers of Paneth cells (*Lyz1*), absorptive cells (*Si*), and goblet cells (*Tff3* and *Chga*). These observations revealed the central role of IL-38 in maintaining the homeostasis of ISCs. In its role in intestinal homeostasis, IL-38 determines the differentiation towards several intestinal cell types, thus explaining the importance of this cytokine in the correct recovery of intestinal injuries.

In order to identify the molecular mechanisms of IL-38 in the intestines, we studied IL-1R9 and IL-1R6, which were identified as putative receptors of IL-38 (5, 10, 12, 13). Intestines taken from IL-38-deficient mice show a significant downregulation of *Fzd5*, *Ephb2*, *Bmpr1a*, *Pdgfra*, *Smoc2*, *Socs3*, *Cdk6*, *Ctca4*, *Olfm4*, *Phlda*, and *Pla2g4a* compared to wild type. On the other hand, we could not see differences in the expression of regenerative genes and IL-36 transcripts in wild type compared to *Il1f10*-deficient mice. This observation highlights the fact that IL-38 ablation

specifically impairs stem cell niche-related expression. Conversely, *Fzd5*, *Bmpr1a*, *Phlda*, and *Cdca7* are the only stem cell markers that appeared significantly downregulated in IL-1R9-deficient mice compared to wild type. *Fzd5* encodes for a Frizzled5 receptor for WNT ligands and crypt proliferation requires it and/or Frizzled8 (45). BMP signaling is essential for driving the correct differentiation of ISCs, and an increasing gradient of BMP from the crypt to the top of the villus determines the proper zonation of intestinal epithelium (46). Among the several receptors of BMP, the one encoded by *Bmpr1a* is important because it regulates the phosphorylation of SMAD1/5/8 in the intestine (26). *Phlda* marks epithelial stem cells (47). *Cdca7* is another marker of ISCs (26). The downregulation of these four transcripts in *Il1rap11*^{-/-} intestines reveals a general disorganization of the intestinal tissue in these mice, but not as dramatic as shown in *Il1f10* knockouts. Moreover, we observed that, using the IL-1R9-deficient mouse, the absence of IL-1R9 does not affect IL-38-dependent increase of organoid size, although IL-1R9 deficiency per se gives rise growth defects. These findings exclude IL-1R9 as a coreceptor for

IL-38, in the intestinal crypt compartment. On the other hand, IL-1R6 silencing resulted in a significant downregulation of organoid size and expression of two stem cell markers (*Fzd5* and *Epbh2*), and the lack of IL-1R6 also blocks the responsiveness of organoids to recombinant IL-38 (Fig. 5). We conclude that IL-1R6 works as IL-38 receptor in the gut stem cell niche compartment.

Another controversial aspect of IL-38 is its nature as a pro- or antiinflammatory cytokine. In most diseased conditions, IL-38 exerts an antiinflammatory function, yet it can induce detrimental effects (10, 48). As regards colorectal cancer, IL-38 was reported to inhibit the ERK pathway and thus suppresses cell migration and proliferation (49). Therefore, given its dual role, IL-38 can be considered as a homeostatic factor that balances the intestine according to its needs. This may also explain why IL-38 works only in a precise concentration range. Upon testing of three different concentrations of IL-38 (2, 20, and 200 ng/mL), only 20 ng/mL induced organoid growth, whereas 2 ng/mL was not sufficient to trigger the IL-38-dependent mechanisms. On the other hand, 200 ng/mL could have saturated the whole receptors necessary for IL-1 signaling, thus inhibiting the effects of IL-1 family members downstream to IL-38. The homeostatic nature of IL-38 was further validated in response to IL-1 β stimulation. In fact, in healthy conditions, IL-38 induces low levels of IL-1 β (about 20 pg/mL) that helped organoids growth. These findings are in line with the discovery of detectable yet low resting circulating concentrations of IL-1 β in healthy patients (50) that are likely necessary to keep the biological systems in a steady state. However, based on our observations in intestinal organoids challenged by high concentrations of IL-1 β or LPS, IL-38 exerts a protective signal that restores the normal conditions and acts as an antiinflammatory cytokine.

All in all, we can conclude that IL-38, by signaling via binding IL-1R6 but not IL-1R9, favors stem cell renewal and differentiation by inducing WNT3a and regulating the expression of crypt-related genes, acting as a growth factor. In this context, IL-38 induces a homeostatic release of IL-1 β (at pg/mL level) that supports growth. On the other hand, in inflamed conditions, IL-38 heals injuries by returning the system to the normal state, again exerting prohomeostatic functions. These observations allow us to conclude that, in the intestine, IL-38 should not be categorized as a pro- or antiinflammatory cytokine, as in different contexts, it can either induce or repress IL-1 β to maintain intestinal homeostasis. These findings are remarkably important if we consider the emerging therapeutic potential of IL-38 (14–16). Our findings revealed that, comparably with what was observed with IL-37, another enigmatic IL-1 family member (51), IL-38 exerts its functions on organoids at a specific concentration. IL-37 and IL-38 are mostly described as antiinflammatory cytokines (52, 53) and recent studies demonstrated that they both can inhibit trained immunity (54–57). In conclusion, our results highlight the importance of IL-38 not only as a growth factor but also as a cytokine that, working only in a specific concentration range, can be a potent modulator of intestinal inflammation in human therapies.

Furthermore, these data highlight the commercial potential of IL-38 as a supplement of commercially available kits for organoids growth: The addition of IL-38 in these kits would increase the culturing efficiency, accelerating growth and crypt budding.

Materials and Methods

Intestinal Crypt Isolation and Organoid Culture. Intestinal segments were collected from wild-type, *Il1f10*-deficient, *Il1rap1*-deficient, and *Nlrp3*-deficient mice and were flushed in cold PBS. Two-cm long Intestinal pieces

were cut longitudinally and washed vigorously for 20 times to remove mucus and debris. Subsequently, tissues were incubated with Gentle Cell Dissociation Reagent (Stemcell Technologies) in a rocking platform for 20 min at room temperature. Cells were removed and intestinal pieces were resuspended in PBS +0.1% BSA and pipetted up and down 10 times. The supernatant was passed through a 70- μ m strainer into a 50-mL tube and centrifuged at 290 \times g for 5 min at 2 to 8 $^{\circ}$ C. Cell pellets were resuspended in DMEM/F-12 with 15 mM HEPES and centrifuged at 200 \times g for 5 min at 2 to 8 $^{\circ}$ C. Isolated crypts in a 50:50 mixture of IntestiCult™ Organoid Growth Medium and Matrigel® and 20 μ L of this solution was transferred to each well of a preheated 24-well plate. The plate was then incubated at 37 $^{\circ}$ C for 15 min and 550 μ L of complete IntestiCult™ Organoid Growth Media was added to each well and changed every 3 d. Organoids were generally passaged every 7/8 d and kept in culture for no more than 3 passages.

In Vivo Models. All the mice used for this study belong to the C57BL/6 genetic strain. Mice were maintained in the same room in ventilated cages (40 to 60 air changes per hour) in 14 h light/10 h dark cycle. Cages are cleaned every 14 d and mouse health are daily checked by facility staff.

Animal protocols were approved by the University of Colorado Animal Care and Use Committee. *Il1f10*-deficient mice (GenBank accession number: NM_153077.2; Ensembl: ENSMUSG00000046845) were generated using CRISPR/Cas9 technology and were previously described in de Graaf et al. (7); *Il1rap1*-deficient mice (GenBank accession number: NM_001160403.1; Ensembl: ENSMUSG00000052372) were generated by deleting Exon 3 using CRISPR/Cas9 technology (Cyagen Biosciences) and were previously described in The et al. (6); the *Nlrp3* knockout mice (B6.129S6-Nlrp3^{tm1Bhk/J}) were purchased from The Jackson Laboratories and previously described in Tengedal et al. (58); the *Il1r1* knockout mice (B6.129S7^{tm1Imx/J}) was kindly provided by Shaikh M Atif.

We decided to use 8-wk-old mice for all the experiments performed. Male *Il1f10*^{-/-}, *Il1rap1*^{-/-}, and *Nlrp3*^{-/-} mice were used for this study. *Il1r1*^{-/-} and their respective controls were female mice.

Protein Extraction and Western Blotting. SIs were collected from wild-type, *Il1f10*-deficient mice. Tissues were lysed in RIPA buffer (Sigma) supplemented with protease and phosphatase inhibitors (Roche) and centrifuged at 13,000 g for 30 min at 4 $^{\circ}$ C, and the supernatants were obtained. Protein concentration was determined in the cleared supernatants using Bio-Rad protein assay (Bio-Rad Laboratories). Electrophoresis was performed on Mini-Protean TGX 4 to 20% gradient gels (Bio-Rad Laboratories) and blotted onto nitrocellulose 0.1- μ m 145 membranes (GE Water & Process Technologies). Membranes were blocked in 5% rehydrated nonfat milk in TBS-Tween 0.5% for 1 h at room temperature. Primary antibody for LGR5 (R&D Systems) was used in combination with peroxidase-conjugated secondary antibodies. A primary antibody against β -Actin (Santa Cruz Biotechnology) was used to assess protein loading.

Mouse IL-38 Expression. A recombinant expression plasmid was ordered from Twist Bioscience (San Francisco, CA) encoding a 6xHis-tagged Small Ubiquitin-Like Modifier (SUMO) followed by mouse IL-38 residues 3 to 152 within pET21b. A typical expression comprised 4 L of luria broth at 37 $^{\circ}$ C with ampicillin selection and induced at 0.6 ODs (600 nM) with isopropyl b-D-1-thiogalactopyranoside for 3 to 4 h. Soluble protein was lysed via sonication and applied to a Ni-affinity resin (Sigma) in Ni-A buffer (50 mM I Na₂HPO₄, pH 7, 500 mM NaCl, 10 mM imidazole) and eluted with Ni-B buffer (50 mM I Na₂HPO₄, pH 7, 500 mM NaCl, 400 mM imidazole). Elutions were dialyzed against Ni-A buffer for subsequent cleavage of the 6xHis-tagged SUMO via recombinant SUMO Protease produced in-house (also known as Ulp1p, UniProt accession A0A0L8VFW2). 6xHis-tagged Sumo was stripped via Ni-affinity, and the untagged IL-38 was concentrated for size-exclusion chromatography using a Superdex-75 column (Cytiva, 120 mL total bed volume) in final buffer (50 mM HEPES, pH 7, 150 mM NaCl). Fractions comprising IL-38 were concentrated and stored at -80 $^{\circ}$ C until further use.

RT-qPCR. Total RNA was extracted from murine SI and from organoid cultures with TRIzol reagent. cDNA synthesis was performed using High-Capacity cDNA Reverse Transcription Kit (Applied Biosystems) according to the manufacturer's protocol. qPCRs were performed in triplicate with SYBR Green Master Mix (Applied Biosystems) by means of QuantStudio 3 Real-Time PCR System (Applied Biosystem). Then, 18s was used as internal standard in each sample. The sequences of the primers used

are listed in *SI Appendix, Table S1*. To reduce the number of mice to sacrifice, we used the same wild-type controls for either *Il1f10* or *Il1rap1*-deficient intestines.

Hematoxylin & Eosin Staining. SI samples were included in paraffin and cut longitudinally. A regressive Hematoxylin and Eosin staining procedure was used. In this method, hematoxylin is applied to the slide followed by an acid differentiating solution to remove excess stain and clarify the nuclear detail. Eosin is then applied to the slide in order to stain the cytoplasm and surrounding structures.

Imaging. Organoid stacks were taken with Olympus IX81 spinning disk after 6 d of culturing. Organoid size was measured using Fiji (ImageJ) software in pixel²; every measurement was normalized with the average of the control group for each experiment.

Immunofluorescence. Mouse intestinal samples were collected and fixed in PBS with 4% paraformaldehyde (Sigma-Aldrich) in PBS. After dehydration, samples were embedded in paraffin molds for sectioning. Sections (5 μm) were obtained and transferred to glass microscope slides. Slides were deparaffinized with xylene and ethanol and permeabilized with 0.1% Tween in TBS solution. After antigen retrieval with citrate buffer, slides were blocked with normal donkey serum and incubated with primary antibodies against LGR5 (clone 803420, Catalog MAB8240, R&D Systems) and IL-38 (catalog ab180898, Abcam) dilution overnight at 4 °C. Alexa flour 647 anti-rat (catalog A48272, Invitrogen) and Alexa flour 488 anti-rabbit at 1:100 (catalog 11008, Invitrogen) were used as secondary antibodies for 1 h at room temperature. Finally, slides were coverslipped in Mowiol mounting media with DAPI. Images were taken using Olympus FV1000 laser scanning confocal/CARS microscope. IL-38 antibody produces massive background probably due to possible cross-reactivity with other interleukins expressed in the intestine (i.e., IL-36a, IL-36b, IL-36g, and IL-36RA). For this reason, a reliable analysis of IL-38 staining can be performed only in comparison with an IL-38 null sample. We tried to use this IL-38 antibody for western blot, but, at least as regards intestinal samples, we could not obtain reliable results.

1. D. M. de Graaf, L. U. Teufel, L. A. B. Joosten, C. A. Dinarello, Interleukin-38 in health and disease. *Cytokine* **152**, 155824 (2022).
2. C. Xie *et al.*, Interleukin-38 is elevated in inflammatory bowel diseases and suppresses intestinal inflammation. *Cytokine* **127**, 154963 (2020).
3. G. Fonseca-Camarillo, J. Furuzawa-Carballeda, E. Iturriaga-Goyon, J. K. Yamamoto-Furusho, Differential expression of IL-36 family members and IL-38 by immune and nonimmune cells in patients with active inflammatory bowel disease. *Biomed. Res. Int.* **2018**, 5140691 (2018).
4. T. Garraud, M. Harel, M.-A. Boutet, B. Le Goff, F. Blanchard, The enigmatic role of IL-38 in inflammatory diseases. *Cytokine Growth Factor Rev.* **39**, 26–35 (2018).
5. F. L. van de Veerdonk *et al.*, IL-38 binds to the IL-36 receptor and has biological effects on immune cells similar to IL-36 receptor antagonist. *Proc. Natl. Acad. Sci. U.S.A.* **109**, 3001–3005 (2012).
6. E. The *et al.*, Interleukin 38 alleviates aortic valve calcification by inhibition of NLRP3. *Proc. Natl. Acad. Sci. U.S.A.* **119**, e2202577119 (2022).
7. D. M. de Graaf *et al.*, IL-38 gene deletion worsens murine colitis. *Front. Immunol.* **13**, 840719 (2022).
8. M. Ohno *et al.*, The anti-inflammatory and protective role of interleukin-38 in inflammatory bowel disease. *J. Clin. Biochem. Nutr.* **70**, 64–71 (2022).
9. A. Huard *et al.*, IL-38 ablation reduces local inflammation and disease severity in experimental autoimmune encephalomyelitis. *J. Immunol.* **206**, 1058–1066 (2021).
10. H. Zhou *et al.*, Interleukin-38 promotes skin tumorigenesis in an IL-1Rrp2-dependent manner. *EMBO Rep.* **23**, e53791 (2022).
11. L. Mermoud *et al.*, IL-38 orchestrates proliferation and differentiation in human keratinocytes. *Exp. Dermatol.* **31**, 1699–1711 (2022).
12. J. Mora *et al.*, Interleukin-38 is released from apoptotic cells to limit inflammatory macrophage responses. *J. Mol. Cell Biol.* **8**, 426–438 (2016).
13. H. Lin *et al.*, Cloning and characterization of IL-1HY2, a novel interleukin-1 family member. *J. Biol. Chem.* **276**, 20597–20602 (2001).
14. W.-D. Xu *et al.*, IL-38, a potential therapeutic agent for lupus, inhibits lupus progression. *Inflamm. Res.* **71**, 963–975 (2022).
15. L. Mercurio *et al.*, IL-38 has an anti-inflammatory action in psoriasis and its expression correlates with disease severity and therapeutic response to anti-IL-17A treatment. *Cell Death Dis.* **9**, 1104 (2018).
16. H. Li *et al.*, Therapeutic effect of IL-38 on experimental autoimmune uveitis: Reprogrammed immune cell landscape and reduced Th17 cell pathogenicity. *Invest. Ophthalmol. Vis. Sci.* **62**, 31 (2021).
17. Q. Wang, L. Ma, C. An, S. G. Wise, S. Bao, The role of IL-38 in intestinal diseases—its potential as a therapeutic target. *Front. Immunol.* **13**, 1051787 (2022).
18. N. Barker *et al.*, Identification of stem cells in small intestine and colon by marker gene Lgr5. *Nature* **449**, 1003–1007 (2007).
19. H. Gehart, H. Clevers, Tales from the crypt: New insights into intestinal stem cells. *Nat. Rev. Gastroenterol. Hepatol.* **16**, 19–34 (2019).
20. A. Haeghebarth, H. Clevers, Wnt signaling, Lgr5, and stem cells in the intestine and skin. *Am. J. Pathol.* **174**, 715–721 (2009).
21. T. Sato *et al.*, Single Lgr5 stem cells build crypt-villus structures in vitro without a mesenchymal niche. *Nature* **459**, 262–265 (2009).

Cytokine Measurements. Cytokine concentrations were measured by specific DuoSet ELISAs (WNT3a and IL-1β) according to the manufacturer's instructions (R&D Systems). Commercially available ELISA kit from R&D Systems was used to detect IL-38 production but we could not obtain reliable results.

Il1rl2 Silencing. *Il1rl2* siRNAs (MBS8235553) and unspecific siRNA as negative control (MBS8241404) were purchased from MyBioSource and transfected with the siTran 2.0 siRNA transfection reagent following the manufacturer's instructions. For transfection, we used 10 nM siRNAs for 24 h. Silencing efficiency was evaluated with RT-qPCR using the *Il1rl2* primers listed in *SI Appendix, Table S1*.

Statistical Analysis. Significance of differences was evaluated with Student's *t* test or one-way ANOVA, where accordingly specified, using GraphPad Prism (GraphPad Software Inc.). Statistical significance was set at *P* < 0.05.

Data, Materials, and Software Availability. All study data are included in the article and/or *SI Appendix*.

ACKNOWLEDGMENTS. We are thankful to Jesper Falkesgaard Højen, Kibrom Meles Alula, Dominik Stich, Elizabeth Kaye, Radu Moldovan for their technical support. A special acknowledgment goes to Fabia Gamboni for her constant and careful support.

Author affiliations: ^aDepartment of Medicine, University of Colorado Anschutz Medical Campus, Aurora, CO 80045; ^bDepartment of Biology, University of Padova, Padova 35121, Italy; and ^cDepartment of Biochemistry and Molecular Genetics, School of Medicine, University of Colorado Denver, Aurora, CO 80045

Author contributions: A.D. and C.A.D. designed research; A.D., M.M., J.A.-A., T.A., J.M.G., C.M., A.T., R.G., J.S.R., W.S.W., S.M.A., and C.A.D. performed research; A.D., J.S.R., S.M.A., S.L., E.Z.E., and C.A.D. contributed new reagents/analytic tools; A.D., M.M., J.A.-A., T.A., J.M.G., C.M., A.T., R.G., J.S.R., W.S.W., S.M.A., S.L., E.Z.E., D.M.d.G., and C.A.D. analyzed data; and A.D., D.M.d.G., and C.A.D. wrote the paper.

22. J. Muñoz *et al.*, The Lgr5 intestinal stem cell signature: Robust expression of proposed quiescent "+4" cell markers. *EMBO J.* **31**, 3079–3091 (2012).
23. K. K. Kumar, A. W. Burgess, J. M. Gulbis, Structure and function of LGR5: An enigmatic G-protein coupled receptor marking stem cells. *Protein Sci.* **23**, 551–565 (2014).
24. K. S. Carmon, X. Gong, Q. Lin, A. Thomas, Q. Liu, R-spondins function as ligands of the orphan receptors LGR4 and LGR5 to regulate Wnt/beta-catenin signaling. *Proc. Natl. Acad. Sci. U.S.A.* **108**, 11452–11457 (2011).
25. J. H. van Es *et al.*, Wnt signalling induces maturation of Paneth cells in intestinal crypts. *Nat. Cell Biol.* **7**, 381–386 (2005).
26. Z. Qi *et al.*, BMP restricts stemness of intestinal Lgr5+ stem cells by directly suppressing their signature genes. *Nat. Commun.* **8**, 13824 (2017).
27. H. Han *et al.*, Loss of aryl hydrocarbon receptor suppresses the response of colonic epithelial cells to IL22 signaling by upregulating SOCS3. *Am. J. Physiol. Gastrointest. Liver Physiol.* **322**, G93–G106 (2022).
28. I. Lukonin *et al.*, Phenotypic landscape of intestinal organoid regeneration. *Nature* **586**, 275–280 (2020).
29. J. Heuberger *et al.*, High Yap and Mll1 promote a persistent regenerative cell state induced by Notch signaling and loss of p53. *Proc. Natl. Acad. Sci. U.S.A.* **118**, e2019699118 (2021).
30. A. Narytnyk *et al.*, Differentiation of human epidermal neural crest stem cells (hEPI-NCSC) into virtually homogenous populations of dopaminergic neurons. *Stem Cell Rev. Rep.* **10**, 316–326 (2014).
31. X.-Y. Zhong *et al.*, Lgr5 positive stem cells sorted from small intestines of diabetic mice differentiate into higher proportion of absorptive cells and Paneth cells in vitro. *Dev. Growth Differ.* **57**, 453–465 (2015).
32. S. Paik, J. K. Kim, P. Silwal, C. Sasakawa, E.-K. Jo, An update on the regulatory mechanisms of NLRP3 inflammasome activation. *Cell. Mol. Immunol.* **18**, 1141–1160 (2021).
33. H. Katsura, Y. Kobayashi, P. R. Tata, B. L. M. Hogan, IL-1 and TNFα contribute to the inflammatory niche to enhance alveolar regeneration. *Stem Cell Rep.* **12**, 657–666 (2019).
34. T. Naito *et al.*, Lipopolysaccharide from crypt-specific core microbiota modulates the colonic epithelial proliferation-to-differentiation balance. *mBio* **8**, e01680–17 (2017).
35. A. M. Hanash *et al.*, Interleukin-22 protects intestinal stem cells from immune-mediated tissue damage and regulates sensitivity to graft versus host disease. *Immunity* **37**, 339–350 (2012).
36. C. A. Lindemans *et al.*, Interleukin-22 promotes intestinal-stem-cell-mediated epithelial regeneration. *Nature* **528**, 560–564 (2015).
37. X. Zhang *et al.*, Interleukin-22 regulates the homeostasis of the intestinal epithelium during inflammation. *Int. J. Mol. Med.* **43**, 1657–1668 (2019).
38. G.-W. He *et al.*, Optimized human intestinal organoid model reveals interleukin-22-dependency of paneth cell formation. *Cell Stem Cell* **29**, 1333–1345 (2022).
39. F. Deng *et al.*, Interleukin-10 expands transit-amplifying cells while depleting Lgr5+ stem cells via inhibition of Wnt and notch signaling. *Biochem. Biophys. Res. Commun.* **533**, 1330–1337 (2020).
40. L. Wang *et al.*, Pro-inflammatory cytokine interleukin-1β promotes the development of intestinal stem cells. *Inflamm. Res.* **61**, 1085–1092 (2012).
41. M. Mahapatro *et al.*, Programming of intestinal epithelial differentiation by IL-33 derived from pericyclic fibroblasts in response to systemic infection. *Cell Rep.* **15**, 1743–1756 (2016).
42. A. T. Mah, K. S. Yan, C. J. Kuo, Wnt pathway regulation of intestinal stem cells. *J. Physiol.* **594**, 4837–4847 (2016).

43. J. Holmberg *et al.*, EphB receptors coordinate migration and proliferation in the intestinal stem cell niche. *Cell* **125**, 1151–1163 (2006).
44. L. G. van der Flier, A. Haegebarth, D. E. Stange, M. van de Wetering, H. Clevers, OLFM4 is a robust marker for stem cells in human intestine and marks a subset of colorectal cancer cells. *Gastroenterology* **137**, 15–17 (2009).
45. Y. Miao *et al.*, Next-generation surrogate Wnts support organoid growth and deconvolute frizzled pleiotropy in vivo. *Cell Stem Cell* **27**, 840–851.e6 (2020).
46. J. Beumer *et al.*, BMP gradient along the intestinal villus axis controls zonated enterocyte and goblet cell states. *Cell Rep.* **38**, 110438 (2022).
47. A. Sakhianandeswaren *et al.*, PHLDA1 expression marks the putative epithelial stem cells and contributes to intestinal tumorigenesis. *Cancer Res.* **71**, 3709–3719 (2011).
48. F. Kinoshita *et al.*, Interleukin-38 promotes tumor growth through regulation of CD8+ tumor-infiltrating lymphocytes in lung cancer tumor microenvironment. *Cancer Immunol. Immunother.* **70**, 123–135 (2021).
49. L. Huang, H. Zhang, D. Zhao, H. Hu, Z. Lu, Interleukin-38 suppresses cell migration and proliferation and promotes apoptosis of colorectal cancer cell through negatively regulating extracellular signal-regulated kinases signaling. *J. Interferon Cytokine Res.* **41**, 375–384 (2021).
50. R. Ter Horst *et al.*, Host and environmental factors influencing individual human cytokine responses. *Cell* **167**, 1111–1124 (2016).
51. S. Li *et al.*, Extracellular forms of IL-37 inhibit innate inflammation in vitro and in vivo but require the IL-1 family decoy receptor IL-1R8. *Proc. Natl. Acad. Sci. U.S.A.* **112**, 2497–2502 (2015).
52. G. Cavalli, C. A. Dinarello, Suppression of inflammation and acquired immunity by IL-37. *Immunol. Rev.* **281**, 179–190 (2018).
53. C. A. Dinarello, The IL-1 family of cytokines and receptors in rheumatic diseases. *Nat. Rev. Rheumatol.* **15**, 612–632 (2019).
54. G. Cavalli *et al.*, The anti-inflammatory cytokine interleukin-37 is an inhibitor of trained immunity. *Cell Rep.* **35**, 108955 (2021).
55. S. Li *et al.*, Role of nuclear interleukin-37 in the suppression of innate immunity. *Proc. Natl. Acad. Sci. U.S.A.* **116**, 4456–4461 (2019).
56. L. U. Teufel *et al.*, Opposing effects of interleukin-36γ and interleukin-38 on trained immunity. *Int. J. Mol. Sci.* **24**, 2311 (2023).
57. D. M. de Graaf *et al.*, IL-38 prevents induction of trained immunity by inhibition of mTOR signaling. *J. Leukoc. Biol.* **110**, 907–915 (2021).
58. I. W. Tengesdal *et al.*, Targeting tumor-derived NLRP3 reduces melanoma progression by limiting MDSCs expansion. *Proc. Natl. Acad. Sci. U.S.A.* **118**, e2000915118 (2021).